AEDC-TR-66-64

CALIBRATION OF THE SHOCK TUNNEL COMPONENT OF COUNTERFLOW RANGE (I) AT MACH 7.5

J. H. Haun and Henry W. Ball

ARO, Inc.

May 1966

VON KÁRMÁN GAS DYNAMICS FACILITY
ARNOLD ENGINEERING DEVELOPMENT CENTER
AIR FORCE SYSTEMS COMMAND
ARNOLD AIR FORCE STATION, TENNESSEE

NOTICES

When U. S. Government drawings specifications, or other data are used for any purpose other than a definitely related Government procurement operation, the Government thereby incurs no responsibility nor any obligation whatsoever, and the fact that the Government may have formulated, furnished, or in any way supplied the said drawings, specifications, or other data, is not to be regarded by implication or otherwise, or in any manner licensing the holder or any other person or corporation, or conveying any rights or permission to manufacture, use, or sell any patented invention that may in any way be related thereto.

Qualified users may obtain copies of this report from the Defense Documentation Center.

References to named commercial products in this report are not to be considered in any sense as an endorsement of the product by the United States Air Force or the Government.

CALIBRATION OF THE SHOCK TUNNEL COMPONENT OF COUNTERFLOW RANGE (I) AT MACH 7.5

J. H. Haun and Henry W. Ball
ARO, Inc.

AF - AEDC
Arnold AFB Tenn

FOREWORD

The work reported herein was sponsored by the Arnold Engineering Development Center (AEDC), Air Force Systems Command (AFSC), Arnold Air Force Station, Tennessee, under Program Element 65402234.

The results of research presented were obtained by ARO, Inc. (a subsidiary of Sverdrup and Parcel, Inc.), contract operator of AEDC under Contract AF40(600)-1200. The test was conducted under ARO Project No. VI3516, and the manuscript was submitted for publication on March 4, 1966.

This technical report has been reviewed and is approved.

Harold L. Rogler
1/Lt, USAF
Aerospace Sciences Division
DCS/Research

Donald R. Eastman, Jr.
DCS/Research

ABSTRACT

Calibration of the shock tunnel component of the Counterflow Range (I) operating with a new nozzle throat designed to yield Mach 7.5 is reported. Transverse pitot-pressure profiles and heat-transfer rates on a hemisphere-cylinder model in the test section were measured at four flow conditions. A single probe was traversed along the nozzle centerline to determine the streamwise pitot-pressure gradient. Shock detachment distances for a hemisphere-cylinder were measured to determine when helium from the shock tunnel driver entered the test section. Results from these tests indicate a repeatable test core of uniform flow having a 12.5-in. diameter. Test times of from 2.5 to 4 msec were recorded before large quantities of helium appeared to be entering the test section. The streamwise pressure measurements indicated a Mach number gradient of 0.2/ft.

CONTENTS

		Page
	ABSTRACT	iii
	NOMENCLATURE	vi
I.	INTRODUCTION	1
II.	APPARATUS	1
III.	DISCUSSION OF RESULTS	2
IV.	CONCLUSIONS	4
	REFERENCES	5

ILLUSTRATIONS

Figure		
1.	Photograph of Pitot-Pressure Rake	7
2.	Photograph of Rake Installation	8
3.	Schematic of Shock Detachment Distance Measurement Apparatus	9
4.	Typical Reservoir and Pitot-Pressure Traces	
	a. $p_o \approx 100$ atm	10
	b. $p_o \approx 700$ atm	11
5.	Summary of the Pitot-Pressure Profile Data	
	a. $p_o \approx 700$ atm	12
	b. $p_o \approx 450$ atm	12
	c. $p_o \approx 225$ atm	12
	d. $p_o \approx 100$ atm	12
6.	Additional Pitot-Pressure Measurements	
	a. Comparison of Mach 11 Pitot Profiles with Previous Calibration Results	13
	b. Streamwise Pitot-Pressure Gradient	13
7.	Comparison of Measured and Theoretical Stagnation Heat-Transfer Rates	14
8.	Comparison of Measured Heat-Transfer Rates at the Shoulder and the Stagnation Point	15
9.	Theoretical Run Time Limits Based upon Arrival of the Helium Driver Gas	16

Figure		Page
10.	Typical Shadowgrams of the Model and Bow Shock. .	17
11.	Summary of the Shock Detachment Distance Measurements	18
12.	Comparison of Experimental and Theoretical Shock Tunnel Run Times	19

TABLES

I.	Summary of Shock Tube Measurements and Computed Stagnation Conditions	21
II.	Summary of Test Section Measurements	22
III.	Summary of Computed Free-Stream Conditions	23

NOMENCLATURE

d	Diameter of driven tube, in.
d*	Throat diameter, in.
h	Enthalpy, ft^2/sec^2
L	Length of driven tube, ft
M	Mach number
p	Pressure, atm
p_o'	Test section pitot pressure, atm
$\dot{q}_o$	Stagnation heat-transfer rate, Btu/ft^2-sec
$\dot{q}_{SH}$	Shoulder heat-transfer rate, Btu/ft^2-sec
R	Model nose radius, in.
Re	Reynolds number, $in.^{-1}$
T	Temperature, °K
t	Time, msec
u	Velocity, ft/sec
z	Distance along the centerline of the tunnel, in.
ρ	Density, amagats
δ	Shock detachment distance, in.

SUBSCRIPTS

1	Initial driven tube charge conditions
4	Initial driver charge conditions
M	Measured
o	Tunnel reservoir conditions
s	Initial shock
T	Theoretical
∞	Free-stream conditions

SECTION I
INTRODUCTION

A calibration test was conducted in the Counterflow Range (I) of the von Kármán Gas Dynamics Facility (VKF) to study the flow conditions in the test section using a large nozzle throat and the highest allowable shock tube charge conditions. This test condition will provide flow at a sufficiently high density to maintain equilibrium conditions in the flow fields of models used during counterflow tests.

The quality of the test section flow was determined from measurements of (1) the transverse pitot-pressure profile, (2) the streamwise pitot-pressure gradient, (3) the stagnation and shoulder heat-transfer rates on a hemisphere-cylinder model, and (4) the time-resolved shock detachment distance on a hemisphere-cylinder model. The shock detachment distance measurements were intended to provide an indication of the arrival of the helium driver gas in the free stream.

The shock tube was operated at tailored interface conditions for room temperature He and air. The maximum driver pressure of 1000 atm produced tunnel reservoir conditions of 1800°K and 700 atm. The reservoir pressure was varied to a minimum of 100 atm during these tests.

SECTION II
APPARATUS

The shock tunnel component of Range I was the same as described in Ref. 1, with the exception that the throat diameter was increased to 1.16 in. in order to produce a high free-stream density test gas. The flow survey rake is shown in Fig. 1. It was mounted in a vertical orientation, and additional probes were positioned 1.75 in. from the top and bottom of the test section, as shown in Fig. 2. Two 1-in.-diam hemisphere-cylinder heat-transfer probes were mounted from the sides of the vertical rake and positioned with axes at 2 and 4 in. from the tunnel centerline.

The rake was instrumented with 50- and 100-psia fast-response, variable reluctance pressure transducers (Refs. 2 and 3). Thermocouple-type heat-transfer gages (Ref. 4) were used at the stagnation points of the heat-transfer probes, and thin-film-type gages were used at the shoulder positions. Reservoir pressures were measured with piezoelectric transducers at stations located 4 and 8 in. upstream of the nozzle throat. These pressures agreed within ±5 percent during each run.

A 2- or a 3-in. -diam hemisphere-cylinder model was used during the phase of the tests in which shock detachment distances were measured. A 16-mm high speed framing camera was used in the arrangement shown in Fig. 3 to take shadowgrams of the model and shock wave.

SECTION III
DISCUSSION OF RESULTS

A complete listing, by run number, of the test conditions covered in this calibration is presented in Tables I, II, and III. Typical reservoir pressure, p_o, and pitot pressure, p_o', traces are shown in Figs. 4a and b. As illustrated in these figures, the period of constant p_o and p_o' decreased with increasing p_o. The constant-pressure period varied from 4 msec at $p_o \approx 100$ atm to 2.5 msec at $p_o \approx 700$ atm.

The pitot profiles which were obtained using the 1.16-in. -diam nozzle throat are presented in Fig. 5. The profiles are flat, within ±10 percent over a 12.5-in. -diam core of flow. The level of the pitot profile was repeatable from run to run within ±10 percent at all test conditions, corresponding to an average Mach number across the core of 7.5.

The pitot profiles which were obtained with the 0.5-in. -diam throat are compared in Fig. 6a to unpublished profiles obtained two years ago during the initial tunnel calibration program. These two sets of data are in good agreement.

The measured streamwise pitot-pressure gradient is shown in Fig. 6b. The gradient in p_o'/p_o of 12 percent per foot, corresponds to a Mach number gradient of 0.2 or 2.5 percent per foot.

In Fig. 7, the measured stagnation heat-transfer rates and theoretical rates based on the Fay and Riddell theory are compared. Seventy-five percent of the data are within ±10 percent of the theoretical values. The agreement implies that the actual total flow enthalpy agrees with the total flow enthalpy calculated from shock tube theory.

The measured heat-transfer rates at the shoulder of the probe are plotted against measured stagnation heating rates in Fig. 8. One point is off considerably, but the bulk of the data lie within ±10 percent of a shoulder-to-stagnation heat ratio of 0.065. Based on the experimentally determined pressure distribution of Ref. 5 (for $M_\infty = 8.1$) and the theory of Lees (Ref. 6), this ratio of heating rates should be 0.065 for the present case.

Figure 9 shows theoretical run times for the Range I shock tunnel, based on the criterion that the run is terminated by the arrival of the He/air interface at the nozzle throat. The curve marked inviscid flow was obtained considering alteration of the shock tube wave diagram (tailored interface conditions) with time as inviscid fluid passes the throat. The set of curves marked viscous flow was obtained considering additional interface acceleration as predicted by Mirels' theory (Ref. 7). For the large throat, d* = 1.16 in., run times of 5.4, 5.7, 6.1, and 6.4 msec were obtained for reservoir pressures of 100, 225, 450, and 700 atm, respectively.

In order to examine experimentally the arrival of helium at the test section, tests were conducted during which the time-resolved shock detachment distance on a spherical-nosed model was photographically recorded. The calculations of Van Dyke and Gordon (Ref. 8) indicate that the detachment distance would increase measurably as the flow changed from pure air to pure helium. Although the Mach number and related quantities are not known when a significant amount of helium enters the test section, it is possible to estimate the limiting shock detachment distance on the basis that, for pure helium behaving as a perfect gas, nozzle expansion area ratio would dictate a maximum Mach number of 15.2, with a corresponding density ratio across a normal shock of 0.253. This Mach number would be reduced by boundary-layer growth on the nozzle walls, but density ratio, and therefore shock detachment distance, would be affected only negligibly. Hence, from Ref. 8, it is found that the detachment distance for pure helium would be 0.20 R.

The shadowgrams in Fig. 10 are typical of those obtained during these tests. During the run chosen for illustration, the detachment distance was nearly constant at 2, 3, and 4 msec but had increased 20 percent at 6 msec. At 10 msec, the model had begun to vibrate and had moved upward in the field of view. Zero time was defined as the instant when the first shock wave appeared at the nose of the model.

The detachment distance data are presented in Fig. 11 in terms of the detachment distance-to-model nose radius ratio as a function of run time. The data show that the detachment distance was erratic during the first 1.5 msec; this period also corresponds to the pitot-pressure rise time (see Fig. 4). For run times between 1.5 and 6 msec, a ±5-percent band is shown for the data to represent its estimated precision. An arbitrary ±5-percent band has also been associated with the theoretical shock detachment distance (Ref. 8) for air. Comparing the ±5-percent bands at the 450-atm condition, for example, it can be noted that during the period 1.5 to 3.5 msec the measured and theoretical shock detachment distances agree, whereas at 5 msec the measured distance is definitely greater than the theoretical value.

By noting similarly restricted run times for the data at all four reservoir pressures, the band marked arrival of helium limit (AEDC-I) in Fig. 12 was obtained. In this figure, the run times from Fig. 11 have been adjusted to a zero time which corresponds to the instant of reflection of the incident shock wave. The adjustment allows the experimental test section run times to be compared with the theoretical shock tube limits shown in Fig. 12. The run times of Fig. 11 were adjusted by adding the nozzle transient time of the starting shock wave (1.0 msec as illustrated by the displacement of the initial rise of the reservoir and pitot-pressure traces in Fig. 4) and subtracting the nozzle transient time of a gas particle during the run (1.4 msec from Ref. 9). The time of initial stabilization and the time of decay of the test section pitot pressure were adjusted in the same manner and are presented in Fig. 12.

The data of Fig. 12 show that at reservoir pressures below 300 atm the Range I run time is definitely limited by the influx of helium rather than by pitot-pressure decay; there is doubt that a helium-free test period exists at these conditions. At a reservoir pressure of 700 atm, however, there is a period of 2 msec during which the pitot pressure will be stable and the shock detachment distance will not differ from the theoretical distance by more than ±5 percent. The arrival of helium limit, obtained indirectly by measuring detachment distances, is shown in Fig. 12 to be in reasonable agreement with the results of experiments at DAL (Ref. 9) and CAL (Ref. 10), obtained directly from time-resolved gas samples. Notice that the present arrival of helium limit band lies 25 to 40 percent below the theoretical viscous flow limit.

SECTION IV
CONCLUSIONS

Tests were conducted in Range I to determine the quality of the shock tunnel flow using a 1.16-in.-diam nozzle throat. The charge pressure of the helium driver gas was varied from 1000 atm, the maximum allowable, to 170 atm, resulting in a variation in nominal tunnel reservoir conditions from 1800°K and 700 atm to 1800°K and 100 atm. From these tests the following conclusions can be drawn:

1. The pitot-pressure distribution was uniform within ±10 percent over a 12.5-in.-diam core of flow.
2. The level of the pitot-pressure profile was repeatable from run to run within ±10 percent. The average Mach number was 7.5, repeatable within ±3 percent.

3. Measurements of stagnation heat-transfer rate on a hemisphere-cylinder probe agreed with theoretical values computed from shock tube conditions within ±10 percent. The agreement implies that the actual total flow enthalpy agrees with the computed total flow enthalpy.

4. The Mach number gradient along the portion of the streamwise axis of the tunnel in the vicinity of the test section was approximately 0.2 per foot.

5. The period of steady pitot pressure varied with tunnel stagnation conditions from 4 msec at the 100-atm condition to 2.5 msec at the 700-atm condition.

6. Measurements of the shock detachment distance on a hemisphere-cylinder model at the high pressure condition, $p_o \approx 700$ atm, agreed with theory within ±5 percent during the period 1.5 to 4 msec after arrival of flow in the test section. During the 4- to 6-msec period, large quantities of helium driver gas entered the test section flow. During tests at the lower pressure conditions, helium appeared to be entering the test section as early as 2.5 msec after the start of flow. The experimentally determined arrival of helium occurred 25 to 45 percent earlier than predicted for viscous flow.

REFERENCES

1. Ball, Henry W. "Initial Operation of the Pilot Counterflow Test Unit (I)." AEDC-TR-65-132 (AD465893), July 1965.

2. Smotherman, W. E. "A Miniature Wafter-Style Pressure Transducer." AEDC-TR-60-11 (AD243875), October 1960.

3. Smotherman, W. E. and Maddox, W. V. "Variable Reluctance Pressure Transducer Development." AEDC-TR-63-135 (AD410171), July 1963.

4. Ledford, R. L. "A Device for Measuring Heat-Transfer Rates in Arc-Discharge Hypervelocity Wind Tunnels." AEDC-TDR-62-64 (AD275740), May 1962.

5. Griffith, B. J. and Lewis, C. H. "A Study of Laminar Heat Transfer to Spherically Blunted Cones and Hemisphere-Cylinders at Hypersonic Conditions." AEDC-TDR-63-102 (AD408568), June 1963.

6. Lees, Lester. "Laminar Heat Transfer over Blunt-Nosed Bodies at Hypersonic Flight Speeds." Jet Propulsion, Vol. 26, No. 4, April 1956, pp. 259-269, 274.

7. Mirels, H. "Shock Tube Test Time Limitation Due to Turbulent Wall Boundary Layer." American Institute of Aeronautics and Astronautics Journal, Vol. 2, No. 1, January 1964, pp. 84-93.

8. Van Dyke, Milton D. and Gordon, Helen D. "Supersonic Flow Past a Family of Blunt Axisymmetric Bodies." NASA Technical Report R-1, 1959.

9. Copper, J. A., Miller, H. R., and Hameetman, F. J. "Correlation of Uncontaminated Test Durations in Shock Tunnels." Fourth Hypervelocity Techniques Symposium, Arnold Air Force Station, November 1965.

10. Bird, K. D., Martin, J. F., and Bell, T. J. "Recent Developments in the Use of the Hypersonic Shock Tunnel as a Research and Development Facility." Third Hypervelocity Techniques Symposium, Denver, March 1964.

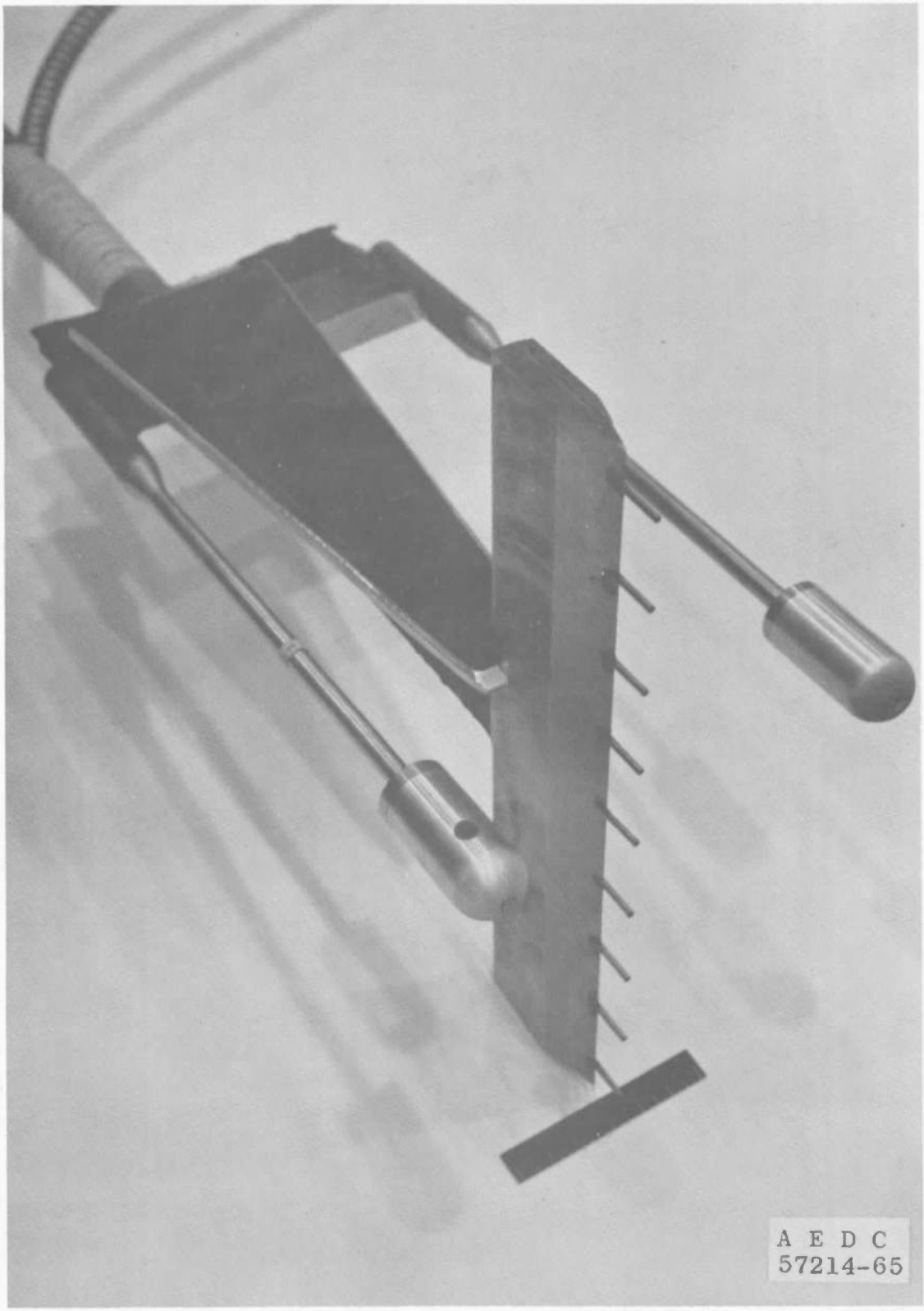

Fig. 1 Photograph of Pitot-Pressure Rake

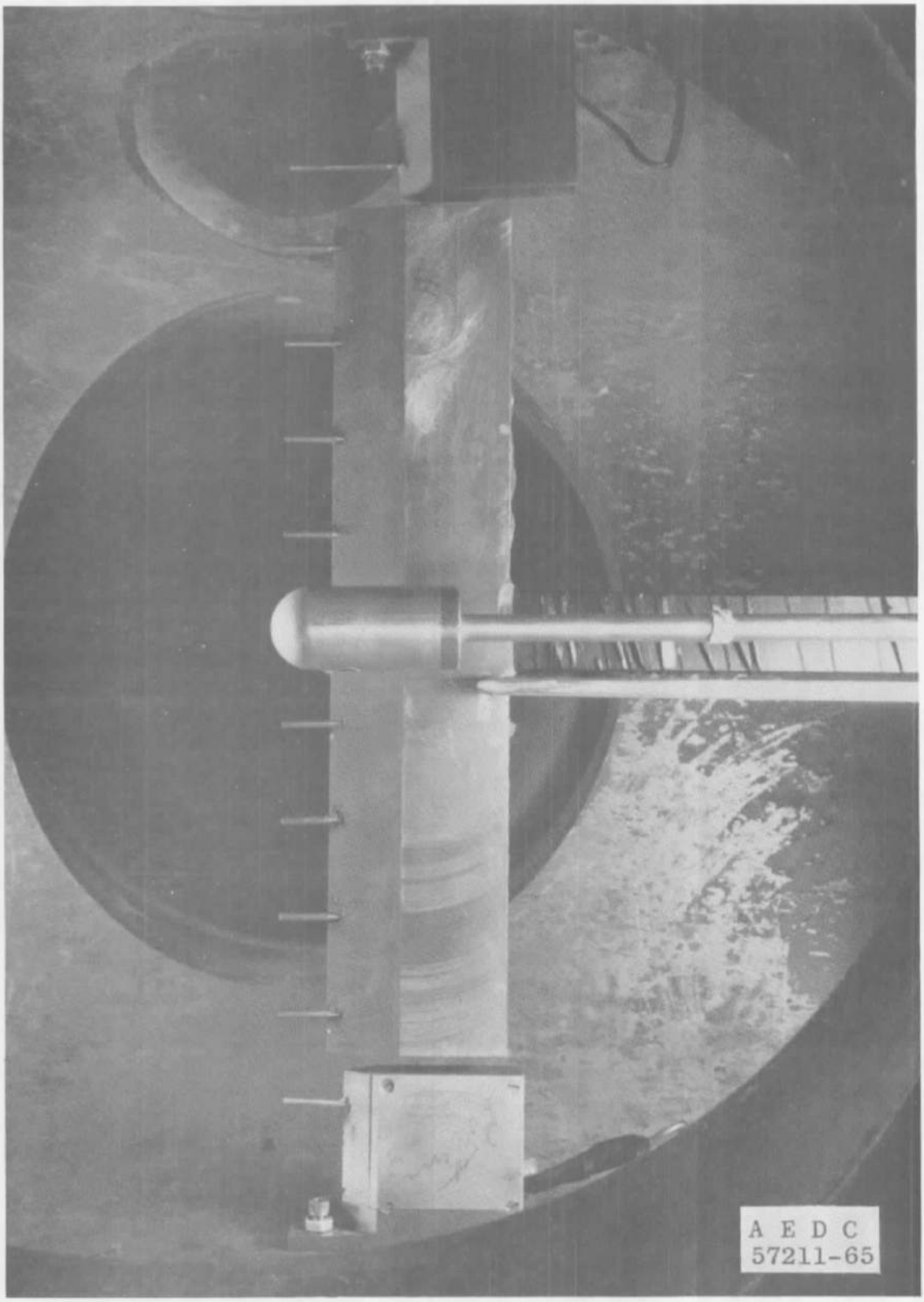

Fig. 2 Photograph of Rake Installation

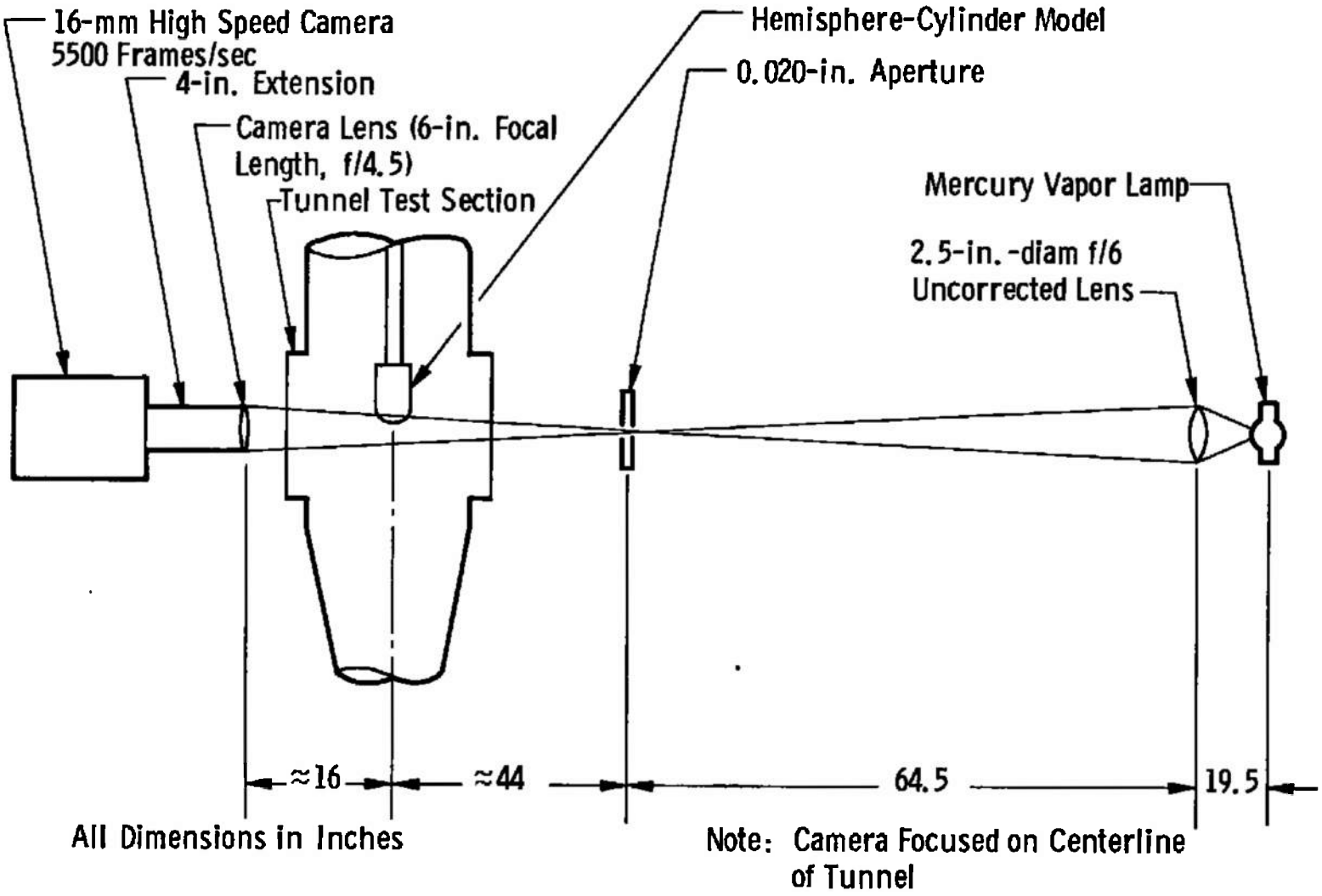

Fig. 3 Schematic of Shock Detachment Distance Measurement Apparatus

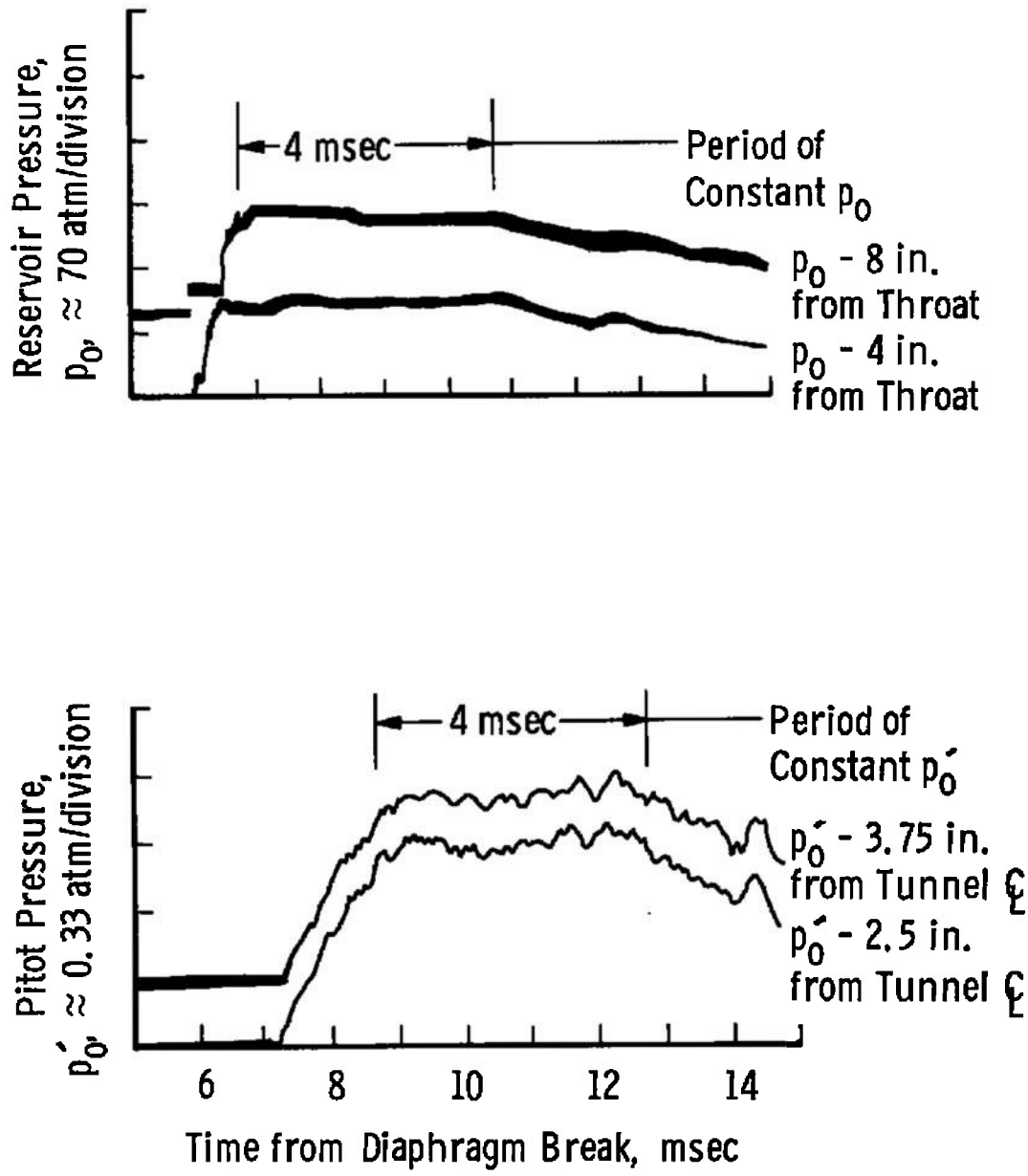

a. $p_o \approx 100$ atm

Fig. 4 Typical Reservoir and Pitot-Pressure Traces

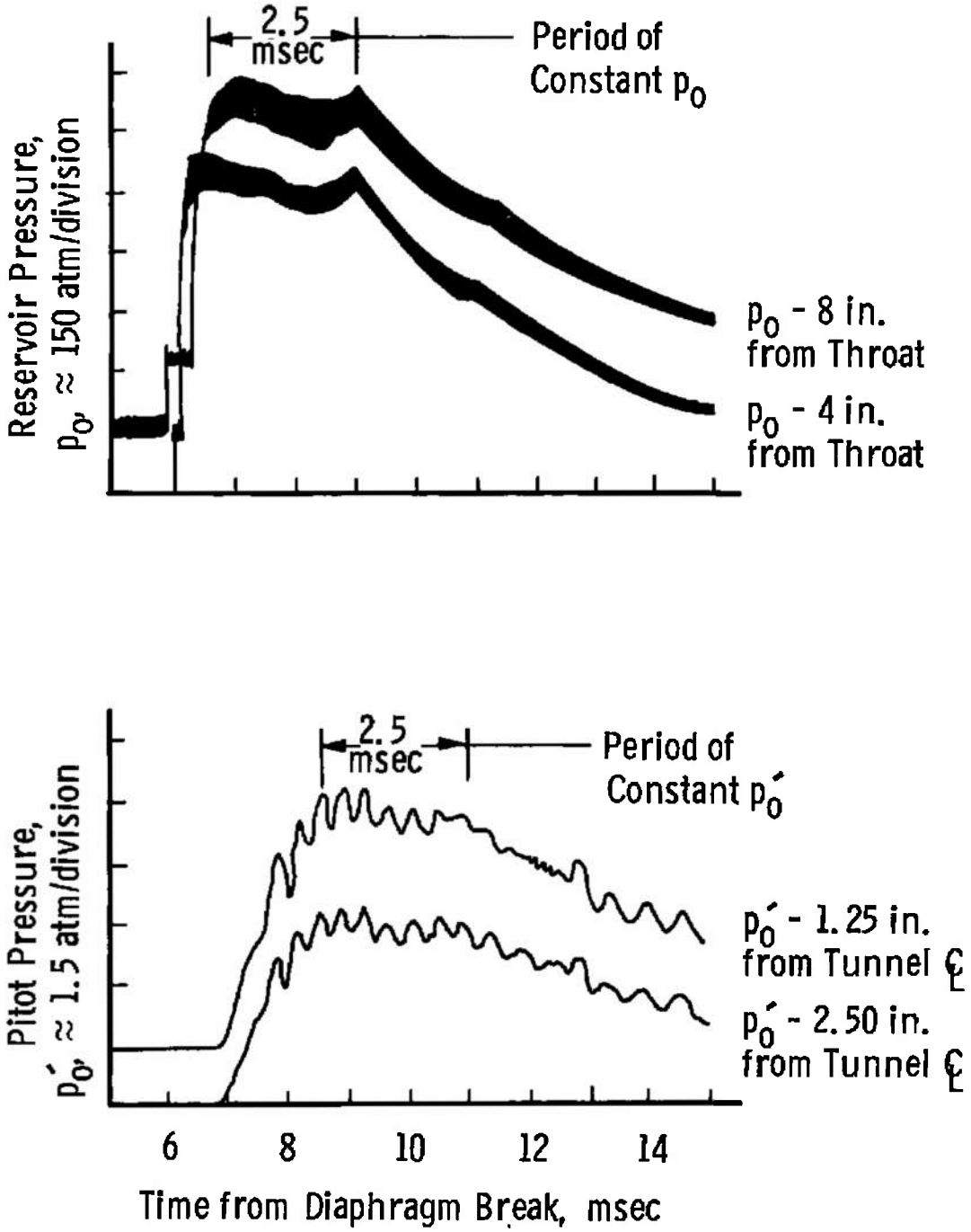

b. $p_o \approx 700$ atm

Fig. 4 Concluded

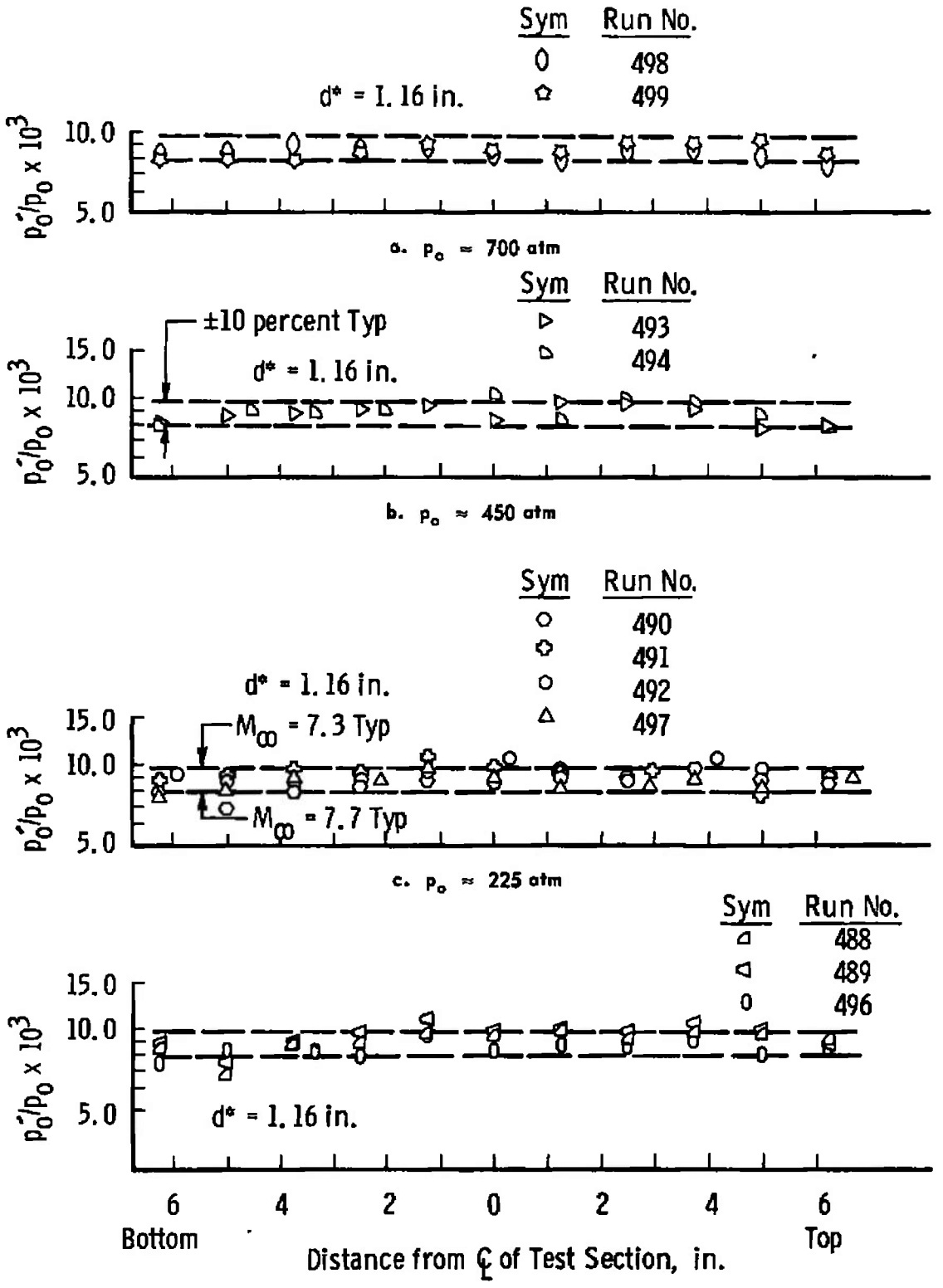

Fig. 5 Summary of the Pitot-Pressure Profile Data

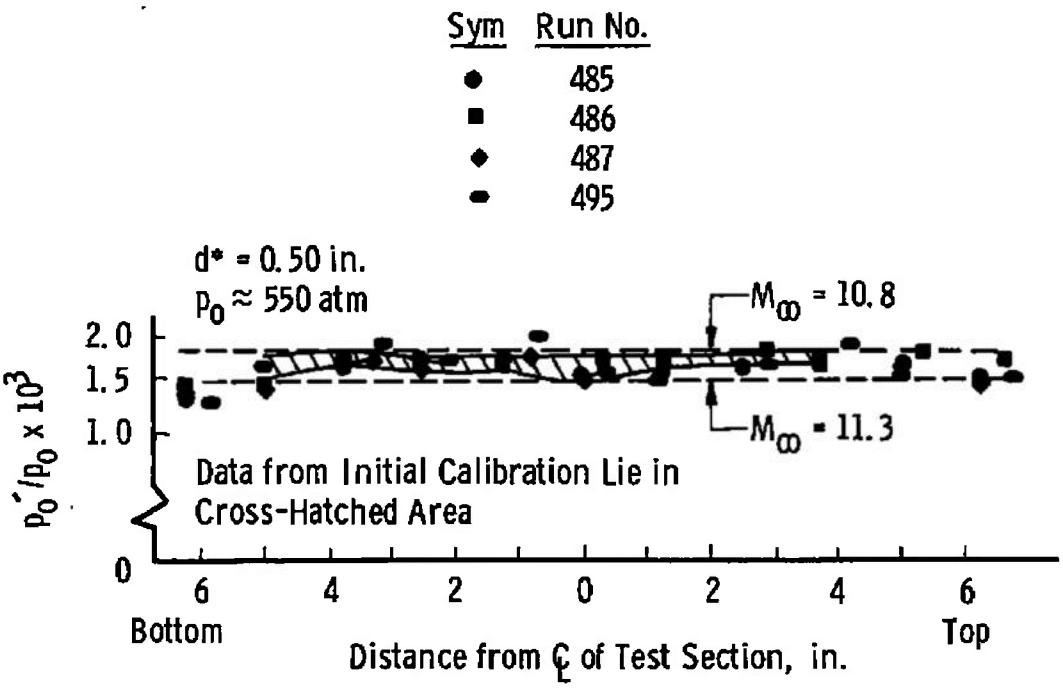

a. Comparison of Mach 11 Pitot Profiles with Previous Calibration Results

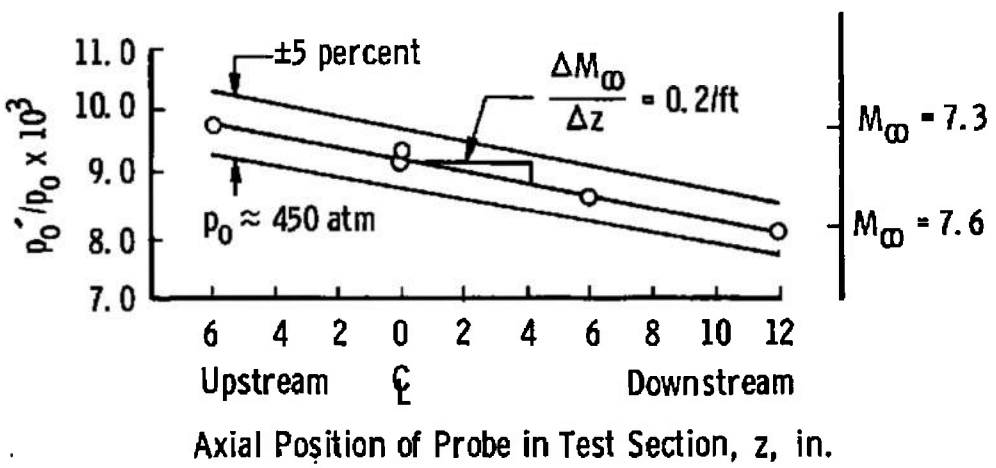

b. Streamwise Pitot-Pressure Gradient

Fig. 6 Additional Pitot-Pressure Measurements

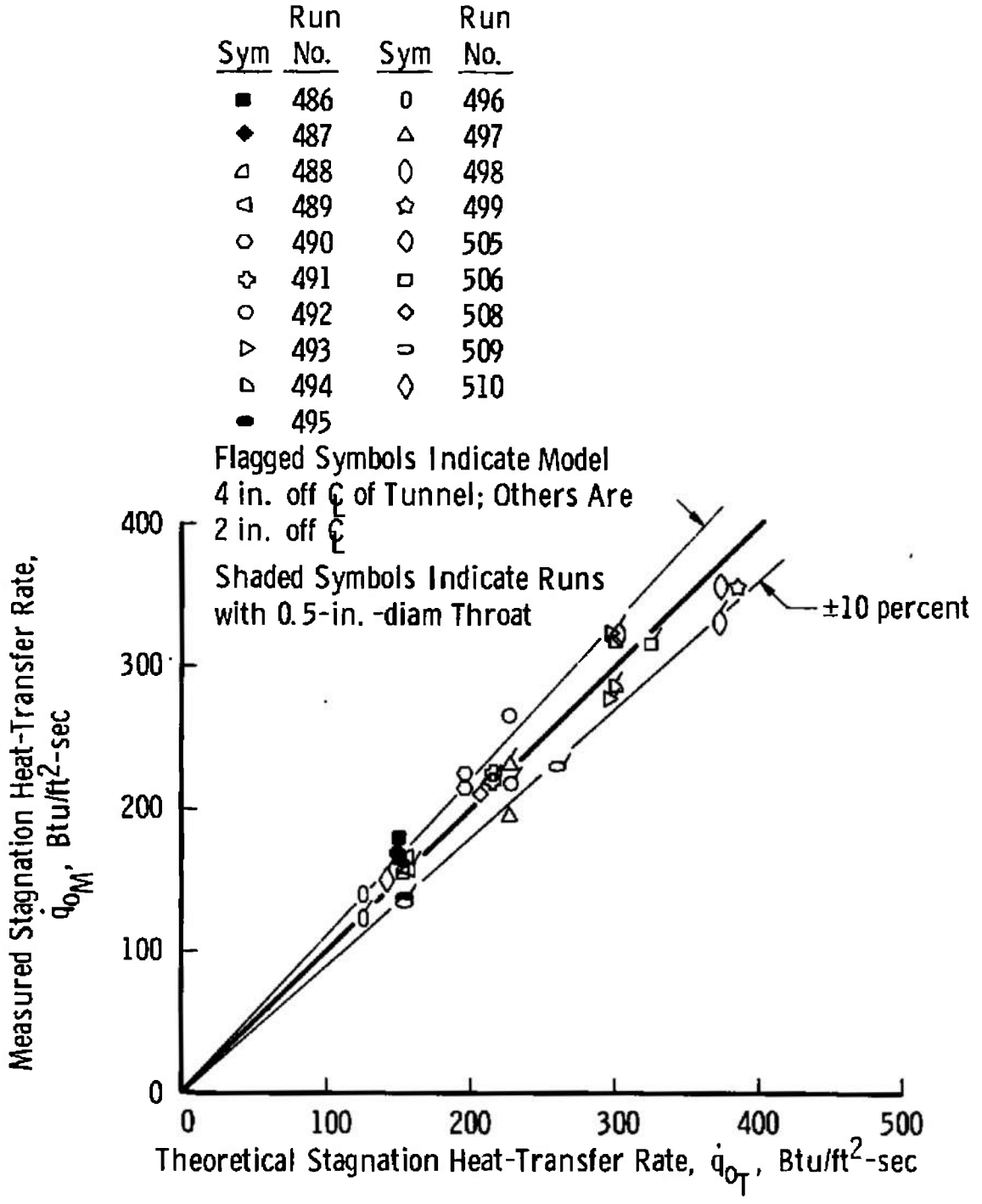

Fig. 7 Comparison of Measured and Theoretical Stagnation Heat-Transfer Rates

Sym	Run No.	Sym	Run No.
◆	487	⊙	496
▱	488	△	497
◁	489	⬯	498
○	490	☆	499
✿	491	◇	505
○	492	◁	507
▷	493	◇	508
▱	494	⬭	509
▬	495	◇	510
		◇	511

Flagged Symbols Indicate Model 4 in. off $\mathcal{C}_L$ of Tunnel; Others Are 2 in. off $\mathcal{C}_L$

Shaded Symbols Indicate Runs with 0.5-in.-diam Throat

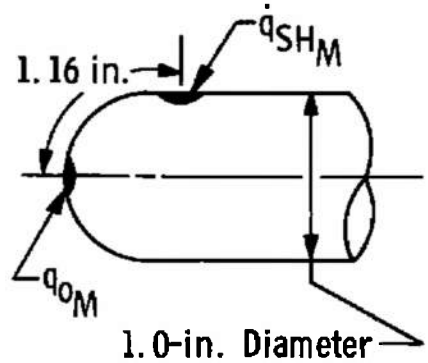

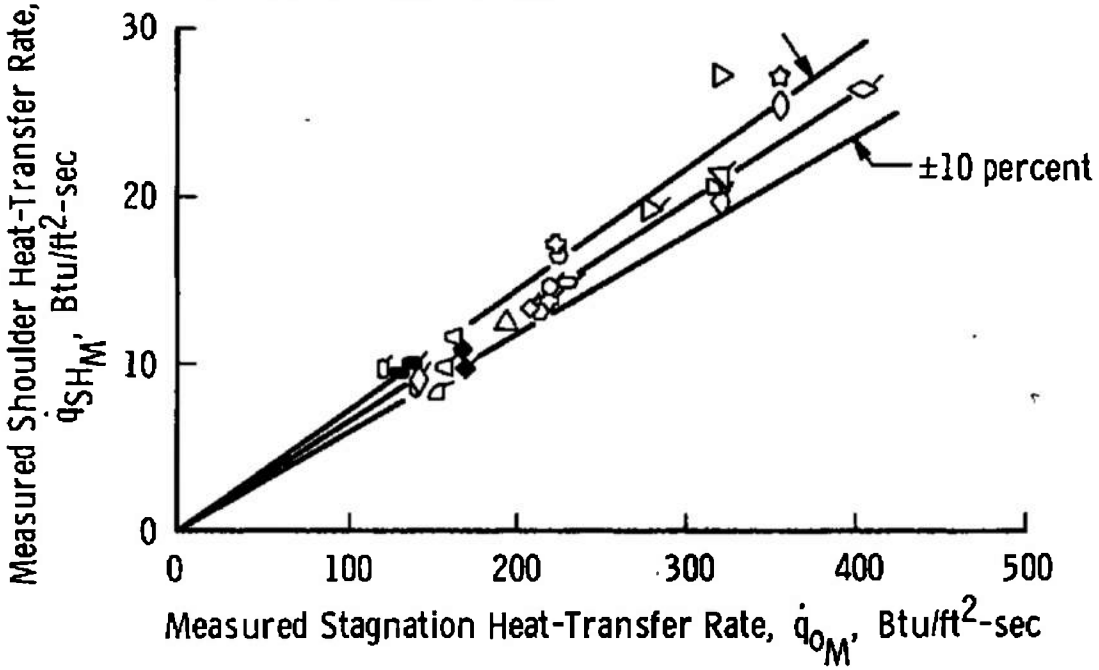

Fig. 8 Comparison of Measured Heat-Transfer Rates at the Shoulder and the Stagnation Point

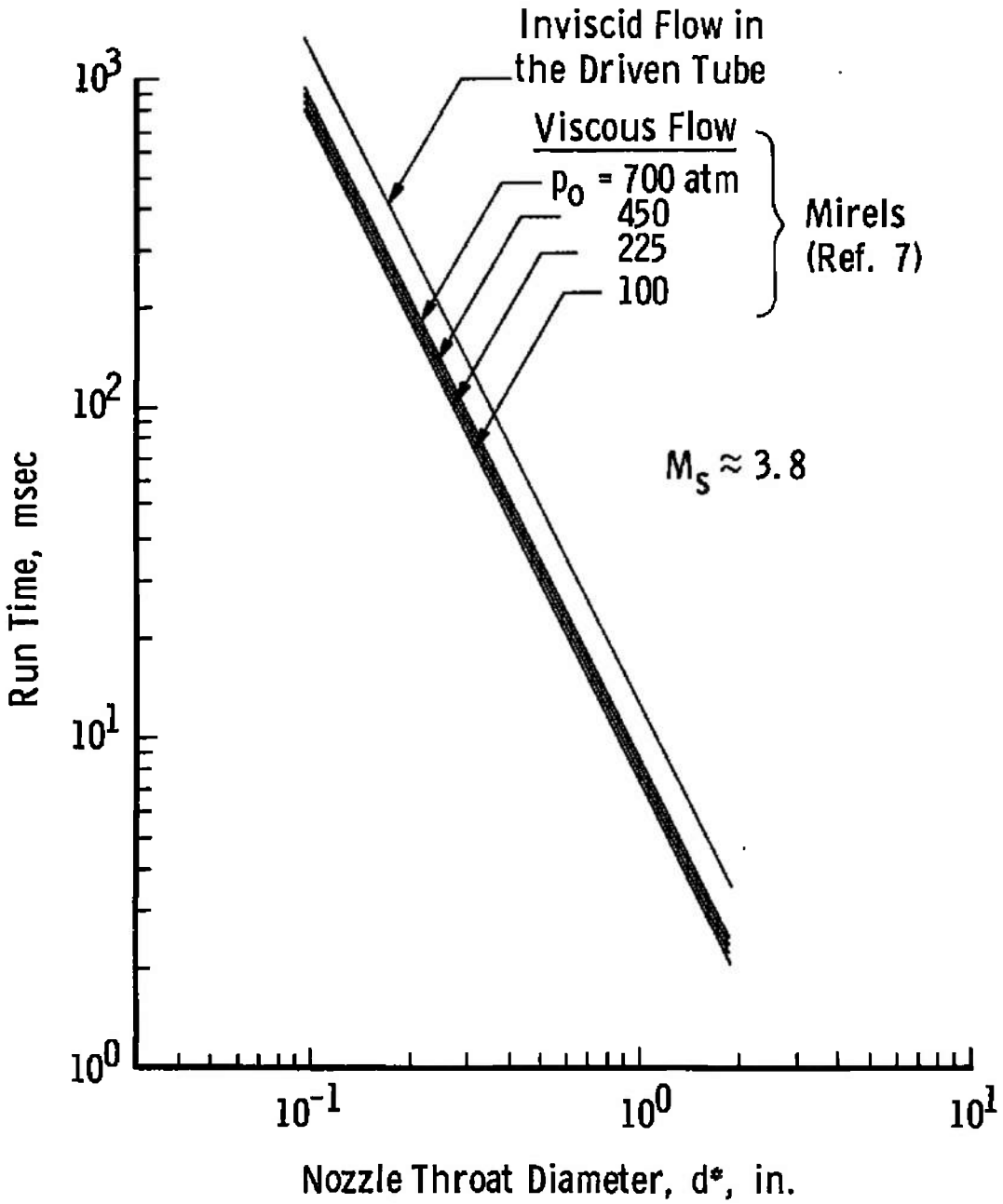

Fig. 9 Theoretical Run Time Limits Based upon Arrival of the Helium Driver Gas

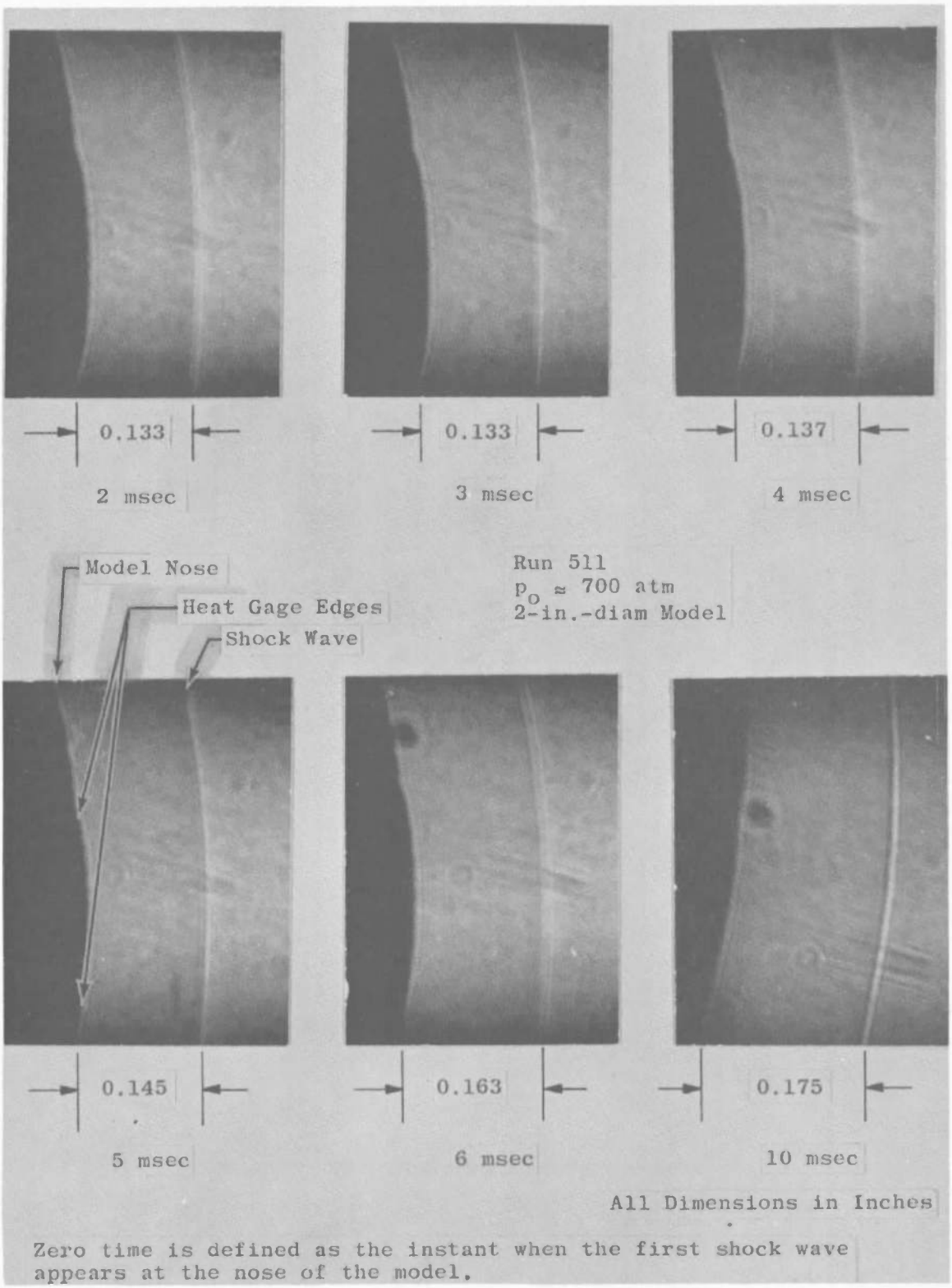

Fig. 10 Typical Shadowgrams of the Model and Bow Shock

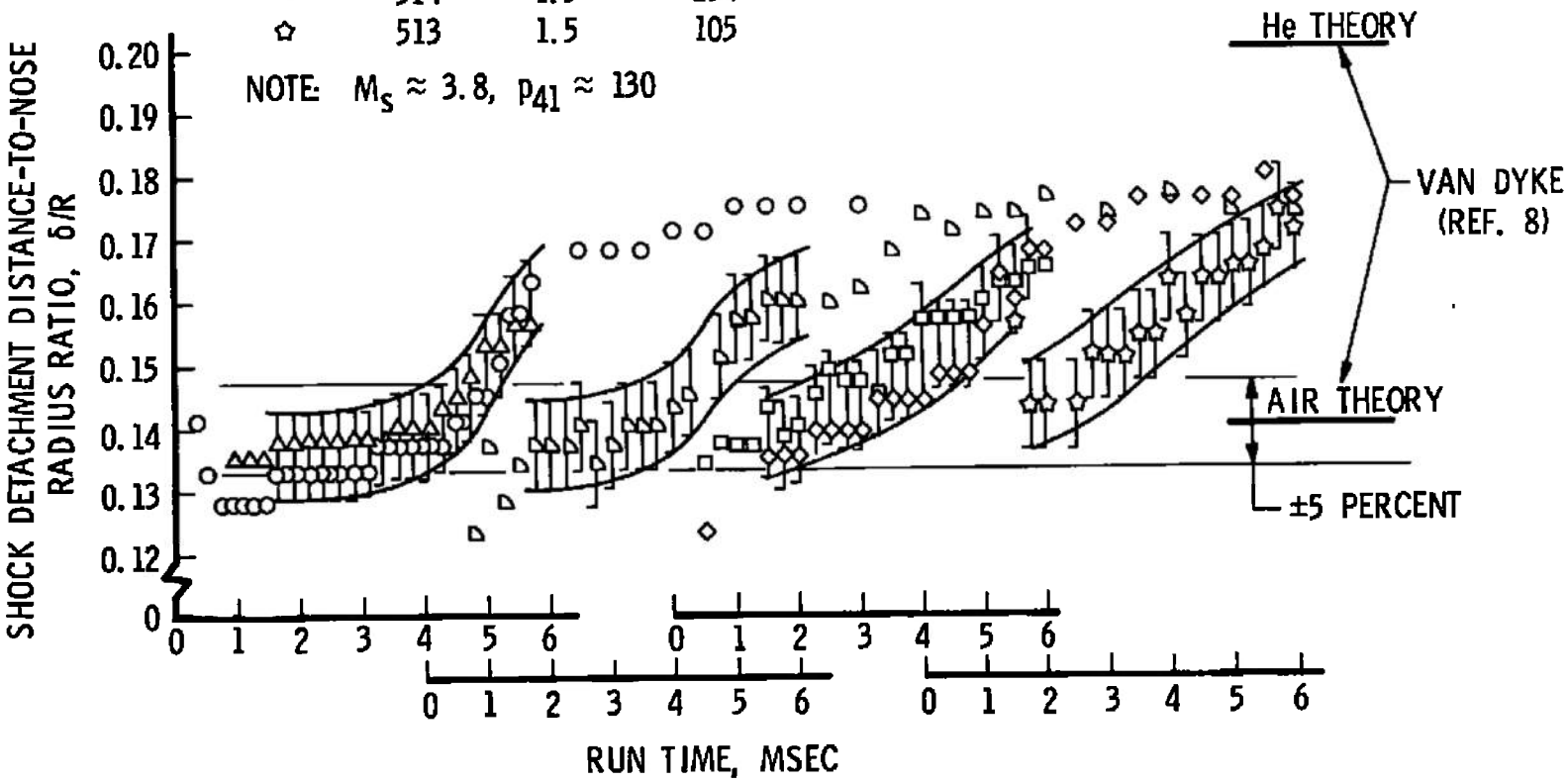

Fig. 11 Summary of the Shock Detachment Distance Measurements

SYM	FACILITY	DRIVEN TUBE LENGTH, L, FT	DRIVEN TUBE DIAM, d, IN.	THROAT DIAM, d*, IN.	d*/d
○	DAL 30 IN. (REF. 9)	31	5	0.84	0.168
□	DAL 30 IN. (REF. 9)	31	5	1.70	0.340
△	CAL 48 IN. (REF. 10)	50	8	1.45	0.168
	AEDC-I	26	3.1	1.16	0.375

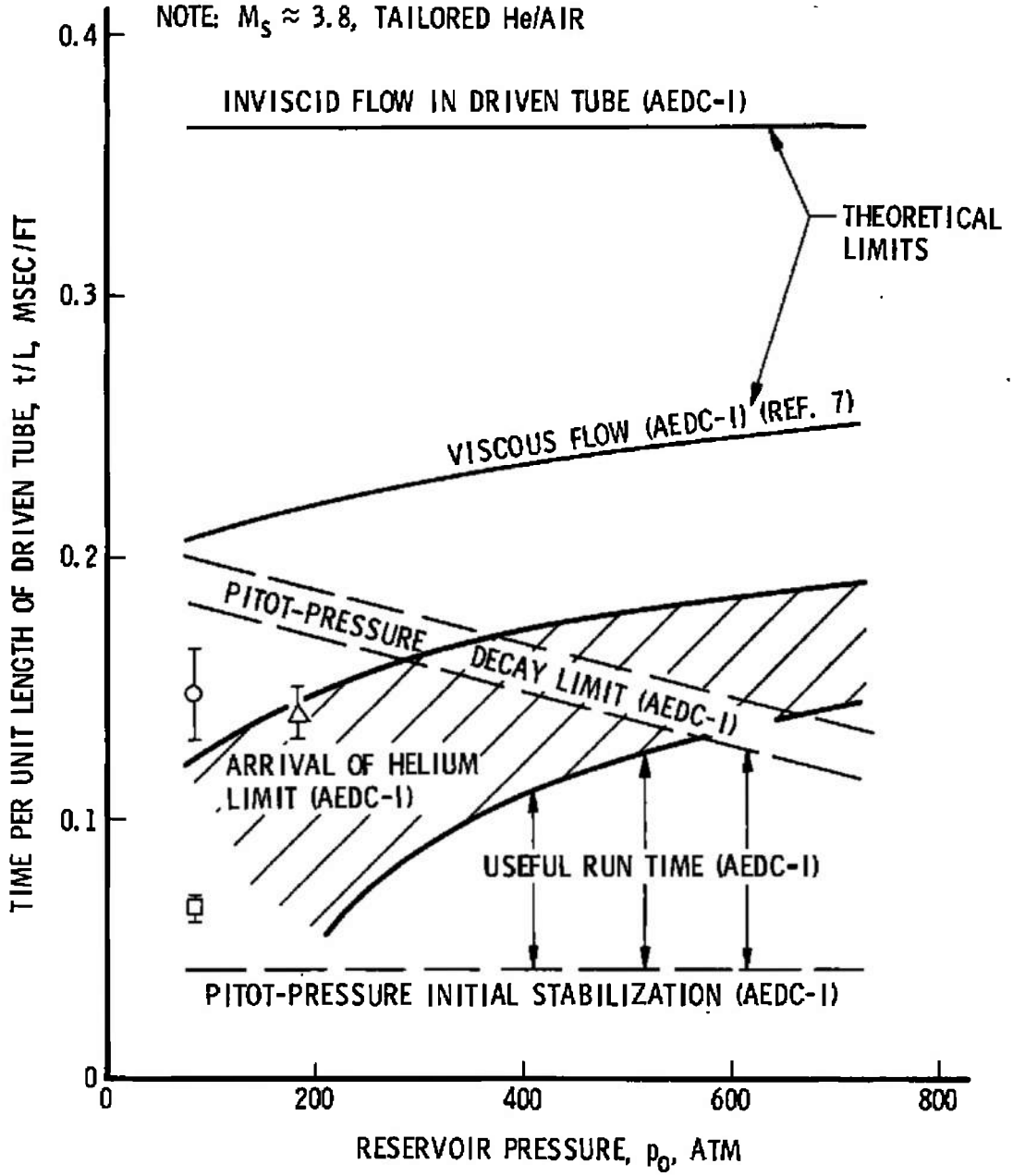

Fig. 12 Comparison of Experimental and Theoretical Shock Tunnel Run Times

TABLE I

SUMMARY OF SHOCK TUBE MEASUREMENTS AND COMPUTED STAGNATION CONDITIONS

Run No.	p_4, atm	p_1, atm	p_2/p_1	M_s	p_o, atm	ρ_o, amg	T_o, °K	h_o, $ft^2/sec^2 \times 10^{-6}$
485	750	5.80	129	3.83	557	74.9	1840	22.8
486	750	5.80	129	3.83	550	74.0	1840	22.8
487	750	5.80	129	3.83	573	77.4	1840	22.8
488	171	1.20	142	3.83	108	15.5	1870	22.8
489	171	1.21	141	3.83	105	14.8	1870	22.8
490	342	2.56	133	3.66	227	32.6	1740	21.5
491	342	2.50	137	3.74	227	33.0	1790	21.9
492	328	2.60	126	3.64	242	33.7	1860	22.8
493	680	5.35	127	3.75	495	63.7	1790	22.0
494	680	5.40	126	3.75	448	62.0	1790	22.0
495	749	5.73	131	3.83	590	79.1	1830	22.8
496	171	1.30	131	3.53	110	17.8	1650	19.8
497	342	2.66	128	3.83	248	37.7	1860	22.8
498	1020	8.05	127	3.84	689	91.0	1830	22.8
499	1020	7.84	131	3.84	702	92.1	1840	23.0
500	680	5.46	125	3.82	441	—	—	—
501	680	5.46	125	3.76	454	—	—	—
502	680	5.46	125	3.79	441	—	—	—
503	680	5.46	125	3.79	441	—	—	—
504	678	5.52	123	3.82	458	—	—	—
505	680	5.46	125	3.86	447	62.9	1790	22.0
506	680	5.45	125	3.83	440	59.3	1870	23.9
507	735	5.60	132	—	475	—	—	—
508	326	2.59	126	3.81	203	29.0	1860	22.8
509	340	2.60	131	3.90	241	31.8	1980	24.5
510	170	1.31	131	3.75	99	14.6	1810	22.0
511	1020	7.40	127	3.84	—	—	—	—
512	170	1.26	136	—	102	—	—	—
513	170	1.34	138	3.76	105	—	—	—
514	340	2.60	131	3.87	234	—	—	—
515	680	5.45	125	3.83	475	—	—	—
516	1020	8.02	127	3.92	690	—	—	—

TABLE II
SUMMARY OF TEST SECTION MEASUREMENTS

Run No.	$(p_o'/p_o)_{avg}$ x 10^3	Model 2 in. from ℄ $\dot{q}_{o_M}$, Btu/ft^2-sec	Model 2 in. from ℄ $\dot{q}_{SH_M}$, Btu/ft^2-sec	Model 4 in. from ℄ $\dot{q}_{o_M}$, Btu/ft^2-sec	Model 4 in. from ℄ $\dot{q}_{SH_M}$, Btu/ft^2-sec	Test Section Arrangement
485	1.67	—	10.6	—	10.0	Pitot Rake and Two Heat Models
486	1.73	179	—	164	—	
487	1.59	169	10.8	170	9.8	
488	8.97	158	—	153	8.1	
489	9.60	164	11.6	159	9.8	
490	8.67	225	16.4	214	13.0	
491	9.47	224	17.1	219	13.8	
492	9.13	264	—	219	14.6	
493	8.19	322	27.3	279	19.1	
494	9.25	317	20.4	286	—	
495	1.67	131	9.5	138	10.0	
496	8.60	140	8.5	122	9.7	
497	8.86	194	12.5	231	—	
498	8.50	356	25.4	330	—	
499	8.68	356	27.1	—	26.8	
500	9.26	—	—	—	—	Single Pitot Probe
501	9.92	—	—	—	—	
502	8.65	—	—	—	—	
503	8.18	—	—	—	—	
504	9.38	—	—	—	—	
505	9.44	—	—	321	19.6	Two-in.-diam Hemisphere-Cylinder, One Heat Model
506	9.65	—	—	310	—	
507	8.84	—	—	322	21.2	
508	8.87	—	—	210	13.1	
509	9.90	—	—	230	14.8	
510	10.6	—	—	142	8.9	
511	—	—	—	405	26.3	
512	10.6	—	—	153	9.1	Three-in-diam Hemisphere-Cylinder, One Heat Model
513	10.6	—	—	150	8.9	
514	9.67	—	—	—	—	
515	9.24	—	—	360	21.2	
516	9.29	—	—	383	25.0	

TABLE III
SUMMARY OF COMPUTED FREE-STREAM CONDITIONS

Run No.	p_∞, atm	ρ_∞, amg	T_∞, °K	u_∞, fps	M_∞	Re_∞, $in.^{-1} \times 10^{-6}$
485	0.0058	0.019	83	6620	11.1	2.65
486	0.0060	0.020	84	6620	11.0	2.68
487	0.0057	0.019	81	6620	11.2	2.70
488	0.0135	0.021	172	6470	7.5	1.43
489	0.0146	0.022	179	6460	7.3	1.44
490	0.0259	0.045	154	6300	7.7	3.22
491	0.0291	0.048	165	6340	7.5	3.28
492	0.0297	0.048	171	6470	7.5	3.19
493	0.0523	0.090	159	6370	7.7	6.35
494	0.0550	0.093	162	6360	7.6	6.37
495	0.0061	0.020	83	6620	11.1	2.82
496	0.0122	0.023	142	6040	7.7	1.74
497	0.0289	0.047	168	6480	7.6	3.2
498	0.0731	0.125	159	6490	7.8	8.95
499	0.0768	0.129	162	6520	7.8	9.15
500	—	—	—	—	7.4	—
501	—	—	—	—	7.3	—
502	—	—	—	—	7.5	—
503	—	—	—	—	7.7	—
504	—	—	—	—	7.4	—
505	0.0560	0.094	162.4	6360	7.6	6.50
506	0.0575	0.090	174.7	6530	7.5	5.95
507	—	—	—	—	—	—
508	0.0238	0.039	167.6	6480	7.6	2.64
509	0.0335	0.048	191.6	6700	7.4	3.00
510	0.0152	0.024	175.6	6340	7.3	1.51

Security Classification

DOCUMENT CONTROL DATA - R&D

(Security classification of title, body of abstract and indexing annotation must be entered when the overall report is classified)

1 ORIGINATING ACTIVITY (Corporate author)	2a REPORT SECURITY CLASSIFICATION
Arnold Engineering Development Center ARO, Inc., Operating Contractor Arnold Air Force Station, Tennessee	UNCLASSIFIED
	2b GROUP N/A

3 REPORT TITLE

CALIBRATION OF THE SHOCK TUNNEL COMPONENT OF COUNTERFLOW RANGE (I) AT MACH 7.5

4 DESCRIPTIVE NOTES (Type of report and inclusive dates)

N/A

5. AUTHOR(S) (Last name, first name, initial)

Haun, J. H. and Ball, Henry W., ARO, Inc.

6 REPORT DATE	7a TOTAL NO OF PAGES	7b. NO OF REFS
May 1966	32	10

8a CONTRACT OR GRANT NO.	9a ORIGINATOR'S REPORT NUMBER(S)
AF40(600)-1200	
b. PROJECT NO.	AEDC-TR-66-64
c Program Element 65402234	9b. OTHER REPORT NO(S) (Any other numbers that may be assigned this report)
d.	N/A

10. AVAILABILITY/LIMITATION NOTICES

Qualified requesters may obtain copies of this report from DDC and distribution of the document is unlimited.

11. SUPPLEMENTARY NOTES	12. SPONSORING MILITARY ACTIVITY
N/A	Arnold Engineering Development Center (AEDC) Air Force Systems Command (AFSC) Arnold Air Force Station, Tennessee

13 ABSTRACT

Calibration of the shock tunnel component of the Counterflow Range (I) operating with a new nozzle throat designed to yield Mach 7.5 is reported. Transverse pitot-pressure profiles and heat-transfer rates on a hemisphere-cylinder model in the test section were measured at four flow conditions. A single probe was traversed along the nozzle centerline to determine the streamwise pitot-pressure gradient. Shock detachment distances for a hemisphere-cylinder were measured to determine when helium from the shock tunnel driver entered the test section. Results from these tests indicate a repeatable test core of uniform flow having a 12.5-in. diameter. Test times of from 2.5 to 4 msec were recorded before large quantities of helium appeared to be entering the test section. The streamwise pressure measurements indicated a Mach number gradient of 0.2/ft.

DD FORM 1 JAN 64 1473

Security Classification

14 KEY WORDS	LINK A		LINK B		LINK C	
	ROLE	WT	ROLE	WT	ROLE	WT
calibration						
shock tunnels						
hypersonic flow						
nozzle						
helium						

INSTRUCTIONS

1. ORIGINATING ACTIVITY: Enter the name and address of the contractor, subcontractor, grantee, Department of Defense activity or other organization *(corporate author)* issuing the report.

2*a*. REPORT SECURITY CLASSIFICATION: Enter the overall security classification of the report. Indicate whether "Restricted Data" is included. Marking is to be in accordance with appropriate security regulations.

2*b*. GROUP: Automatic downgrading is specified in DoD Directive 5200.10 and Armed Forces Industrial Manual. Enter the group number. Also, when applicable, show that optional markings have been used for Group 3 and Group 4 as authorized.

3. REPORT TITLE: Enter the complete report title in all capital letters. Titles in all cases should be unclassified. If a meaningful title cannot be selected without classification, show title classification in all capitals in parenthesis immediately following the title.

4. DESCRIPTIVE NOTES: If appropriate, enter the type of report, e.g., interim, progress, summary, annual, or final. Give the inclusive dates when a specific reporting period is covered.

5. AUTHOR(S): Enter the name(s) of author(s) as shown on or in the report. Enter last name, first name, middle initial. If military, show rank and branch of service. The name of the principal author is an absolute minimum requirement.

6. REPORT DATE: Enter the date of the report as day, month, year; or month, year. If more than one date appears on the report, use date of publication.

7*a*. TOTAL NUMBER OF PAGES: The total page count should follow normal pagination procedures, i.e., enter the number of pages containing information.

7*b*. NUMBER OF REFERENCES: Enter the total number of references cited in the report.

8*a*. CONTRACT OR GRANT NUMBER: If appropriate, enter the applicable number of the contract or grant under which the report was written.

8*b*, 8*c*, & 8*d*. PROJECT NUMBER: Enter the appropriate military department identification, such as project number, subproject number, system numbers, task number, etc.

9*a*. ORIGINATOR'S REPORT NUMBER(S): Enter the official report number by which the document will be identified and controlled by the originating activity. This number must be unique to this report.

9*b*. OTHER REPORT NUMBER(S): If the report has been assigned any other report numbers *(either by the originator or by the sponsor)*, also enter this number(s).

10. AVAILABILITY/LIMITATION NOTICES: Enter any limitations on further dissemination of the report, other than those imposed by security classification, using standard statements such as:

(1) "Qualified requesters may obtain copies of this report from DDC."

(2) "Foreign announcement and dissemination of this report by DDC is not authorized."

(3) "U. S. Government agencies may obtain copies of this report directly from DDC. Other qualified DDC users shall request through _____."

(4) "U. S. military agencies may obtain copies of this report directly from DDC. Other qualified users shall request through _____."

(5) "All distribution of this report is controlled. Qualified DDC users shall request through _____."

If the report has been furnished to the Office of Technical Services, Department of Commerce, for sale to the public, indicate this fact and enter the price, if known.

11. SUPPLEMENTARY NOTES: Use for additional explanatory notes.

12. SPONSORING MILITARY ACTIVITY: Enter the name of the departmental project office or laboratory sponsoring *(paying for)* the research and development. Include address.

13. ABSTRACT: Enter an abstract giving a brief and factual summary of the document indicative of the report, even though it may also appear elsewhere in the body of the technical report. If additional space is required, a continuation sheet shall be attached.

It is highly desirable that the abstract of classified reports be unclassified. Each paragraph of the abstract shall end with an indication of the military security classification of the information in the paragraph, represented as *(TS), (S), (C), or (U)*

There is no limitation on the length of the abstract. However, the suggested length is from 150 to 225 words.

14. KEY WORDS: Key words are technically meaningful terms or short phrases that characterize a report and may be used as index entries for cataloging the report. Key words must be selected so that no security classification is required. Identifiers, such as equipment model designation, trade name, military project code name, geographic location, may be used as key words but will be followed by an indication of technical context. The assignment of links, rules, and weights is optional.